NMR Spectroscopy of Adsorbed ^{129}Xe at Low Temperatures and High Magnetic Fields

J. D. O'Neill, E. V. Krjukov, and J. R. Owers-Bradley
School of Physics and Astronomy, University of Nottingham, Nottingham, NG7 2RD, England

Y. Xia
School of Chemistry, University of Nottingham, Nottingham, NG7 2RD, England
(Dated: August 1, 2006)

In this paper we report measurements of the nuclear magnetic resonance (NMR) spectrum of ^{129}Xe adsorbed on silica gel and Grafoil substrates in a 15 tesla magnetic field and temperatures in the range 10 mK to 1 K. Liquid ^{3}He is used to shorten the longitudinal relaxation time the ^{129}Xe spins and obtain a high degree of spin polarization of over 40% in around a day. The ^{129}Xe NMR spectrum generally exhibits two lines. We show that one line corresponds to the monolayer of surface xenon atoms and the other line to the monolayers of bulk solid xenon between the substrate and the surface monolayer. By comparing the spectra and relaxation rates for xenon of different ^{129}Xe concentrations and by adding ^{4}He we were able to investigate the ^{129}Xe interlayer coupling. The work has important implications in the study of porous materials using hyperpolarized gases, the study of surface atoms by NMR and the production of hyperpolarized species by the brute force technique.

PACS numbers:

I. INTRODUCTION

Polarized noble gases are frequently used as contrast agents in NMR studies. ^{129}Xe in particular, has proved to be a powerful tool in the field of spectroscopy. Its electron shell, which is the largest of all the stable noble gases, is readily polarized in the presence of other atoms and leads to chemical shifts exceeding 7000 ppm in compounds [1] and up to 300 ppm in its elemental state [2]. That, twinned with its chemical inertness, has made it a particularly useful probe in the investigations of mesoporous materials such as porous silicas [3, 4], silica microspheres [5], alumina-silicas [6], clays [7] and, more frequently, zeolites [8, 9]. Recent advances in the production of hyperpolarized ^{129}Xe have refined its use as a probe [10, 11, 12], dramatically increasing its sensitivity and allowing the investigation of materials with relatively small surface areas such as graphitized carbon [2] and even single crystal surfaces [13, 14].

Surface studies often concentrate on the chemical shift of the ^{129}Xe NMR resonance line from a reference frequency to obtain information regarding the surface structures and states of adsorption sites. The interpretation of the chemical shift is usually based upon the suggestions of Ito and Fraissard [9].

$$\delta = \delta_0 + \delta_{Xe} + \delta_s \tag{1}$$

where δ_0 is the chemical shift due to the diamagnetic shielding of the nucleus by its surrounding electron shell, δ_{Xe} is the shift due to Xe - Xe interactions and δ_s is due to the interaction between the Xe and the surface atoms of the substrate. δ_0 or reference chemical shift is the observable gas line extrapolated to zero pressure and has been observed to shift the ^{129}Xe NMR line by 5600 ppm compared to naked ^{129}Xe nuclei [15, 16]. The contributions of δ_{Xe} and δ_s are paramagnetic and are related to the reduction in shielding due to perturbations in the electron shell through interactions with the xenon's local environment.

NMR investigations of solid xenon at very low temperatures are normally difficult because of the exceedingly long spin-lattice relaxation time [17]. In order to encourage relaxation, paramagnetic oxygen impurities have been applied to solid xenon [16, 18, 19] with some success. However, in 2003 Biškup *et al* [20] showed that liquid ^{3}He, when condensed over solid adsorbed xenon, could be an effective ^{129}Xe relaxant. We have used this relaxation method throughout the work reported here.

In our previous paper [19] we showed that the NMR spectrum from solid xenon adsorbed on to silica gel consisted of two distinct lines and interpreted this within a layered model of xenon atoms. We treated the surface xenon monolayer and xenon within the lower monolayers separately, each subject to a different chemical shift. This idea is supported by the fact that the xenon chemical shift, due to Xe−Xe interaction, is dominant over the interaction with other atoms [21] and independent of the concentration of xenon isotopes [16].

Here we report the measurements of the NMR signal from xenon adsorbed on substrates of silica gel (60 Å and 150 Å) and exfoliated graphite and investigate the coupling between the surface ^{129}Xe atoms and the ^{129}Xe atoms in the lower monolayers in attempt to understand the relaxation mechanisms and NMR spectra of xenon at low temperatures and high magnetic fields.

II. EXPERIMENT

The experimental setup for these investigations was identical to the apparatus used in our earlier work, as described in [19]. The experiments involved four different cells containing either silica or Grafoil substrates. Cell I - 1.40 g of Merck Silica gel, 70-230 mesh, main pore size 60 Å; Cell II - 1.81 g of Merck Silica gel, 35-60 mesh, main pore size 150 Å; Cell III - 2.62 g of the same material as in Cell I; Cell IV - 3.19 g of Grafoil® (exfoliated graphite). The properties of the four samples and the results of our measurements of the surface area for each of them are summarized in Table I. The coverage of xenon was calculated by following the assumption of Terskikh *et al* [3] and Conner *et al* [5], that the surface area occupied by each xenon atom was 18 $Å^2$.

The most important characteristics of the substrate, the total surface area and the pore size, were determined by a conventional volumetric technique using a Micromeritics ASAP2020 sorptometer. Before analysis the samples were oven dried at 150 °C and evacuated for 12 hours at 250 °C under vacuum. The surface area was calculated using the BET method based on nitrogen adsorption at 77 K, in the partial pressure (P/P_0) range 0.05 to 0.2. The pore size distribution was obtained by using the BJH adsorption isotherm branch the results of which can be seen on Fig. 1 and summarized in Table I. The distribution of pore sizes for Grafoil is more or less constant and is evidence of a non-porous structure. For the silica gels, it can be clearly seen that the largest contribution to the surface area is from the main pore size quoted by the manufacturers.

The NMR experiments were performed with the cell inside the mixing chamber of an Oxford Instruments KelvinoxTLM dilution refrigerator. Cell I was made from Macor, a low proton ceramic. All other cells were made from Stycast 1266 epoxy resin. Natural xenon (24.6% ^{129}Xe) was used in cells I, II and IV and isotopically enriched xenon (86% ^{129}Xe) was used in cell III. Once mounted on the TLM probe, each substrate was annealed at a temperature of 130 °C and pressure of $<10^{-2}$ mbar for 24 hours. The adsorption of xenon onto the substrates was performed in two different ways. In the first method, a large 2 litre volume containing 300 mbar of xenon gas was used. The amount of gas condensed onto the substrate was then measured by monitoring the small change in pressure in the large volume while the temperature of the cell was slowly reduced from 200 K to 160 K. In the second method, a small calibrated volume (18 cm^3) containing xenon at 1000 mbar was used to condense portions of xenon at cell temperatures of around 175 K. In each case a heated capillary was used to prevent blockages by frozen xenon during this transfer process. As noted above, the ^{129}Xe spin-lattice relaxation times were shortened by condensing liquid ^{3}He into the cell at 1 K, immersing the substrate. Free induction decay signals, following short 5 μs NMR tipping pulses (corresponding to a rotation of $\sim 4°$), were used to monitor the magnetization growth following saturation by large angle rf tipping pulses. A magnetic field of **around** 14.7 T was used corresponding to a ^{129}Xe Larmor frequency of around 165 MHz. We were able to cool the xenon to below 10 mK but most of the experiments were conducted at a temperature of 100 mK. **We can not specify exactly the shift in our data with respect to δ_0 as defined in Eq. 1 because there is no gas present at the temperatures of our experiments, nor can we use solid xenon as a reference, since previous studies have measured a range of values for the shift for bulk xenon [16, 18]. The data displayed in this paper is referenced to the signal generator of our spectrometer, the magnetic field being variable. We believe the observed NMR spectral lines, from the adsorbed solid xenon, are centered at approximately +300 ppm above δ_0.**

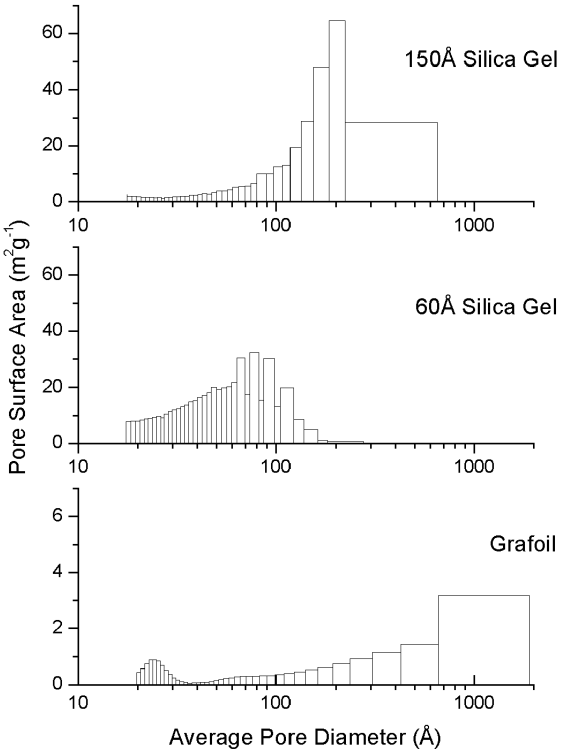

FIG. 1: A histogram of the distribution of surface area over pore size for each substrate from the BJH adsorption isotherm branch.
Upper 150 Å silica gel - BET Surface Area = 313 m^2g^{-1}, middle 60 Å silica gel - BET Surface Area = 516 m^2g^{-1}, lower Grafoil - BET Surface Area = 19.8 m^2g^{-1}.

TABLE I: Cell and Substrate Details

Cell	Material	Appearance	Mean Pore Size (Å)	Mass (g)	Total Surface Area (m^2)	Xenon Coverage (monolayers)	^{129}Xe (%)
I	Merck Silica Gel	70 − 230 mesh, powder	60	1.40	650	0.60 1.40	24.6
II	Merck Silica Gel	35 − 60 mesh, powder	150	1.81	553	0.72 1.63	24.6
III	Merck Silica Gel	70 − 230 mesh, powder	60	2.62	1217	0.74 1.51	86.0
IV	Grafoil®	126 discs: 13mm dia 0.1mm thick		3.19	53.6	0.82 1.82	24.6

A. Cooling the Xenon

In our previous paper [22] we showed that the growth of the magnetization of the surface xenon nuclei at extremely low temperatures was governed by two factors:

i. the dipole-dipole coupling between the ^{129}Xe and the ^{3}He nuclei.

ii. the length of time to cool the xenon to the temperature of the helium refrigerant in the surrounding mixing chamber.

We have seen that at temperatures below 100 mK the second time is much longer than the first. We concluded that the dominant thermal resistance, between the helium refrigerant in the mixing chamber and the xenon in the sample cell, was the Kapitza resistance at the cell walls. To reduce this thermal resistance we redesigned the sample cell for the experiments with Cell III. We constructed the base of the cell from 0.2 mm thick copper with a 2 mm layer of silver sinter attached to both sides to act as a heat exchanger. A comparison of temperature measurements from inside the sample cells is shown on Fig. 2.

In the case of Cell II, the temperature was measured by the amplitude of the equilibrium NMR signal from ^{27}Al, 10^{-3} moles of which had been placed inside the cell prior to cooling. With the isotopically enriched xenon, used in Cell III, the amplitude of the equilibrium xenon NMR signal could be used as a thermometer. In both cases reference measurements of the NMR signals were taken at 1K. It can be clearly seen on Fig. 2 that the sinter greatly improves the thermal contact between the mixing chamber and the xenon. It was possible, under these conditions, to cool the xenon in the cell to a temperature of 10mK and polarize the ^{129}Xe to its equilibrium value (40%) within 24 hours. **Note, for the xenon NMR initially the signal was sampled every 5 minutes. This interval was increased to every hour until the final point which had an interval of 21 hours and 44 minutes. This last point shows that the pulses themselves did not significantly affect the temperature being measured.**

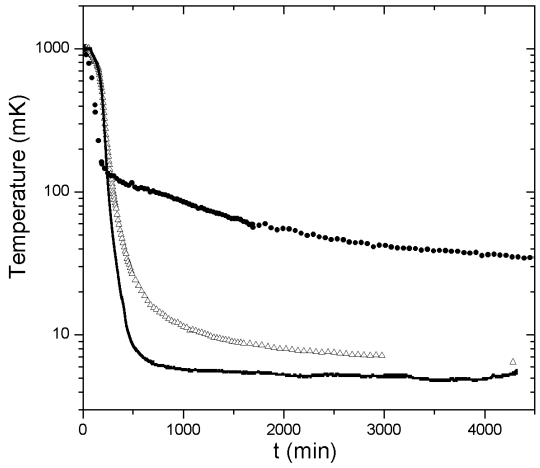

FIG. 2: Sample Cell Internal Temperature: • stycast sample Cell II using ^{27}Al NMR, △ stycast sample Cell III with heat exchanger using ^{129}Xe NMR, Solid Line - temperature of mixing chamber, **measured using a calibrated RuO resistor.**

III. RESULTS AND DISCUSSION

A. Cell I - 60 Å Silica Gel

It should be noted that some results from this substrate have already been presented earlier [19]. It can be seen in Fig. 3 that the NMR signal from the ^{129}Xe has two lines, each fitting well to a Lorentzian curve. The areas under each of the curves correlated with our calculated values of surface coverage by the xenon. In general we suppose that the left line is the spectral component from the surface monolayer of xenon atoms (henceforth denoted as $^{129}Xe_{Surface}$); the right line from the xenon atoms contained within the lower monolayers (henceforth denoted as $^{129}Xe_{Bulk}$), that is, xenon with bulk-like properties. The $^{129}Xe_{Bulk}$ atoms will have the greatest number of

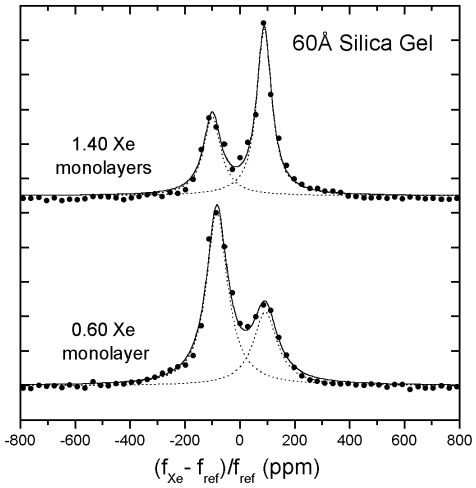

FIG. 3: Normalized ^{129}Xe NMR spectra from natural xenon adsorbed onto 60 Å silica gel at 100 mK, Cell I.

^{129}Xe-^{129}Xe interactions as well as a higher density and as a result the Larmor frequency for these atoms is shifted to a higher frequency due the reduction in electron shielding.

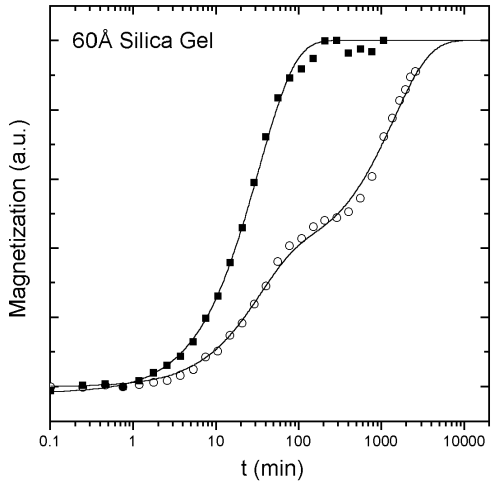

FIG. 4: Magnetization growth of ^{129}Xe adsorbed onto 60 Å silica gel at 100 mK, Cell I: ■ 0.60 monolayers, ○ 1.40 monolayers of natural xenon.

Substantiating behavior for our theory on the origin of the spectrum is evident in the magnetization growth, plotted on Fig. 4. For a coverage of 0.60 monolayers (mostly surface atoms) there appears to be a simple exponential growth. It is evident that the magnetization growth from a coverage of 1.4 monolayers of xenon consists of two components with quite different relaxation times. The surface xenon monolayer, which is in direct contact with the ^{3}He, has a much shorter relaxation time than the lower or bulk layers. This shows that the $^{129}Xe_{Surface}-^{129}Xe_{Bulk}$ interlayer coupling is clearly weaker than the coupling of the surface monolayer to the liquid ^{3}He.

It should be noted that the xenon spectrum from 0.60 xenon monolayers, seen on Fig. 3, also has a significant second line. This suggests that the xenon forms islands with 2 or more atomic layers rather than an ideal single monolayer on this substrate, a scenario already seen by Pietrass *et al* [4].

The width of each of the spectral lines (Fig. 3) was around 25 kHz, much wider than the dipole width for natural xenon **found by others [13, 18]. The broad line width originates from variations in the distribution of xenon atoms on the silica gel surface. These variations result in irregular Xe - Xe interactions producing a non-uniform chemical shift. Inhomogeneities in the local magnetic field from the applied magnetic field, as well as from the substrate and the ^{3}He also contribute to the broad spectral lines. It's of interest to note that the spectral line associated with the bulk xenon was consistently narrower than the surface spectral line in samples that exceeded 1 monolayer. Indeed the width of the bulk spectral line was inversely related to the number of monolayers adsorbed, consistent with our ideas that the line originated from a regularly ordered, bulk like solid.**

B. Cell II - 150 Å Silica Gel

To investigate the dependence of the results on the choice of substrate, the next experiments were performed on a substrate with a substantially larger average pore size, 150 Å. The results are presented on Fig. 5 and Fig. 6. Splitting in the NMR spectrum by the same frequency is evident again. For a sub-monolayer coverage, the NMR spectrum was dominated by the lower frequency line (95% of the signal) in contrast to the 60 Å silica gel, suggesting a more uniform distribution of xenon across the surface (Fig. 5). **When 1.63 monolayers were adsorbed the spectrum consisted of two lines. The larger peak is associated with $^{129}Xe_{Bulk}$ (the ratio of the areas under each of the curves was $^3/_4$) giving further evidence of a non-uniform deposition of xenon during adsorption, as seen with 1.40 monolayers on Cell I.**

The magnetization growth curves for the 150 Å silica gel are presented on Fig. 6. As with the 60 Å gel, with sub-monolayer coverage, the magnetization growth fitted well to a single exponential (solid squares). When a greater amount of xenon was adsorbed (open circles),

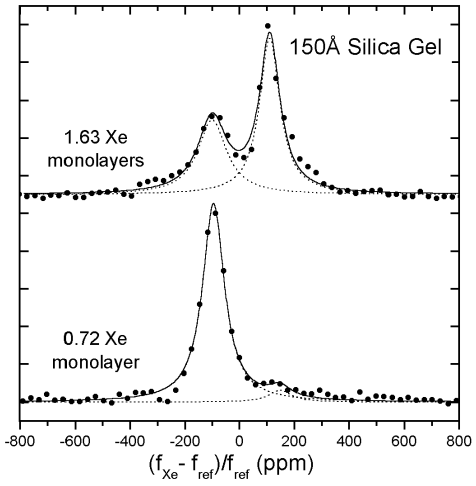

FIG. 5: Normalized ^{129}Xe NMR spectra from natural xenon adsorbed on to 150 Å silica gel at 100 mK, Cell II.

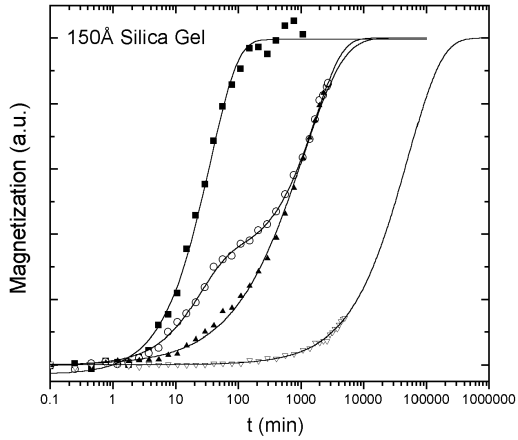

FIG. 6: Magnetization growth of natural ^{129}Xe adsorbed on to silica gel, Cell II: ■ 0.82 monolayers and ∘ 1.63 monolayers of xenon with ^{3}He, ▲ 1.63 monolayers with ^{3}He and ^{4}He, ▽ 1.63 monolayers with ^{4}He only.

two components in the growth curve were clearly seen.

In our previous experiments with 60 Å silica gel [19] we showed that admittance of ^{4}He into the sample cell dramatically increases relaxation time of the surface xenon. The ^{4}He binds more easily to the substrate than the ^{3}He and creates a solid monolayer between the ^{3}He and the xenon thereby reducing the magnetic coupling and increasing the relaxation time by about a factor of 20. The ^{3}He$-^{129}$Xe coupling varies as r^6, where r is the interatomic spacing. Similarly, when only ^{4}He was added to Cell II, the relaxation rate of surface ^{129}Xe, became much longer.

One interpretation of the data could be that a fraction of the small pores are blocked with frozen xenon leading to decoupling and a much longer relaxation time for these spins. The data on Fig. 6 do not support this suggestion. Had the right hand spectral line (denoted $^{129}Xe_{Bulk}$) originated from xenon inside blocked pores we would expect those spins to relax at about the same rate as the ^{129}Xe with only ^{4}He present (the slowest growing magnetization on Fig. 6). Instead, the magnetization growth of $^{129}Xe_{Bulk}$ is much faster than this. Careful analysis of NMR signal amplitude shows that the existence of spins with a much longer relaxation time can be ruled out. There are two possible scenarios that would enable the $^{129}Xe_{Bulk}$ to relax so quickly: either the $^{129}Xe_{Bulk}$ interacts with ^{3}He directly (with the coupling between the surface and bulk xenon restricted due to difference in Larmor frequencies) or relaxation occurs through the dipole - dipole coupling between the surface and bulk xenon atoms and only the $^{129}Xe_{Surface}$ atoms interact with the ^{3}He. Further investigations with isotopically enriched xenon lead us to believe that the second scenario is the more probable as explained below.

C. Cell III - 60 Å Silica Gel with Enriched Xe

60 Å silica gel was used as a substrate for isotopically enriched xenon where the concentration of the ^{129}Xe isotope was 86%. The idea behind these experiments was to examine what effect changing the ^{129}Xe density has on the $^{129}Xe_{Surface}-^{129}Xe_{Bulk}$ coupling. If the two xenon spectral lines belong to physically separated adsorption sites on the surface of the substrate, there would be only weak dipole coupling between the spins at different sites. Increasing the ^{129}Xe isotope concentration would have little effect on the spin-lattice relaxation times of the two components. If instead, the two lines belonged to surface and bulk xenon respectively, as in our model, then any $^{129}Xe_{Surface}-^{129}Xe_{Bulk}$ coupling would be a function of the ^{129}Xe concentration. It follows that this could lead to a shorter T_1 for the $^{129}Xe_{Bulk}$. It can be seen by comparing Fig. 3 and Fig. 7 that the main spectral features are very similar for the natural xenon and the isotopically enriched xenon.

The NMR lines in Fig. 7 are well resolved and each line fits well to a Lorentzian curve. We were able to measure the magnetization growth and spin-lattice relaxation time, T_1, for each component. The results of this analysis are summarized in Table II. It is evident, that compared to natural xenon (26% ^{129}Xe) the relaxation time for the right hand line ($^{129}Xe_{Bulk}$) is shorter and the relaxation time for the left hand line ($^{129}Xe_{Surface}$) line is longer for the enriched xenon. This is clearly seen in the ratios **of the bulk and surface** T_1s and is attributed to an increase in $^{129}Xe_{Surface}-^{129}Xe_{Bulk}$ coupling. It demonstrates that while the atoms contributing to the two lines

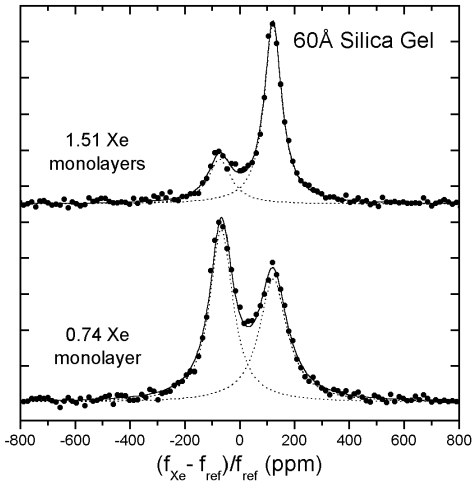

FIG. 7: Normalized ^{129}Xe NMR spectra from enriched xenon adsorbed onto 60 Å silica gel at 100 mK, Cell III.

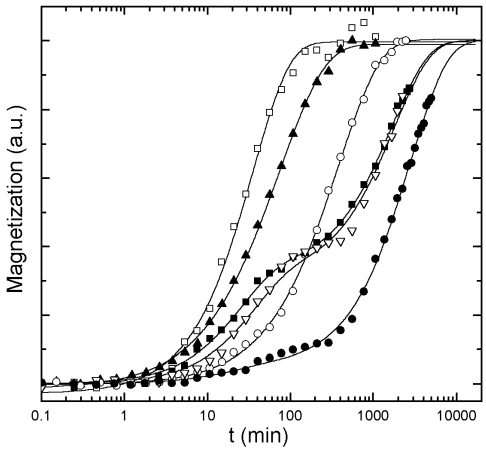

FIG. 8: Magnetization growth curves for ^{129}Xe on the silica gel substrates. ▽ 1.40 and • 3.00 monolayers of natural xenon on 60 Å silica gel, □ 0.72 monolayers and ■ 1.63 monolayers of natural xenon on 150 Å silica gel, ▲ 0.74 monolayers and ○ 1.51 monolayers of enriched xenon on 60 Å silica gel.

are in close proximity to each other, the coupling is not sufficient to induce an increase in overlap of the lines.

Detailed on Fig. 8 are magnetization growth curves for xenon adsorbed on the silica gels. The curves relating to 1.40 monolayers of natural xenon on 60 Å silica gel and 1.63 monolayers on 150 Å silica gel are very similar; the relaxation due to the bulk and the surface atoms are clearly visible. The small differences in relaxation times between similar amounts of xenon condensed on different substrates could be because the ^{3}He can permeate more readily through adsorbents with larger pore sizes. For ***the 3.00*** monolayers of xenon, the fast relaxing component is barely visible; the curves are normalized and the amplitude of the $^{129}Xe_{Bulk}$ signal is greater than the $^{129}Xe_{Surface}$ signal.

There is little evidence for two relaxation rates in case of the isotopically enriched xenon, emphasizing the stronger interaction between surface and bulk ^{129}Xe compared to natural xenon. **The faster relaxation rate of the 0.72 monolayers of natural xenon in comparison with 0.74 monolayers of enriched xenon suggests that cross relaxation with ^{131}Xe as seen by [17] is still occurring at these high B/T conditions, although it could also be due to the greater quantity of ^{129}Xe in the sample.**

To examine more closely the interlayer coupling in the ^{129}Xe, one of the spectral lines was saturated while monitoring the effect this had on the spectrum. Strong coupling would be indicated by the two lines maintaining their relative amplitudes. Isotopically enriched xenon adsorbed onto 60 Å silica gel (Cell III) was allowed to relax to a thermal equilibrium polarization at 100 mK. The frequency of the receiver, f_{ref}, was set to the $^{129}Xe_{Bulk}$ frequency (right hand line). A polarization destroying comb of low amplitude 50 μs pulses, at the frequency of the $^{129}Xe_{Surface}$ atoms ($f_{ref} - 240$ ppm), was applied at regular intervals to saturate the majority of surface spins. The bandwidth of this pulse was small enough prevent the excitation of the $^{129}Xe_{Bulk}$ atoms. During this process the NMR signal from the total system was monitored with short, high amplitude tipping pulses at the reference frequency. It can be seen on Fig. 9 that excitation of the $^{129}Xe_{Surface}$ leads to saturation of the whole spectrum indicating a strong coupling between spin systems. To verify that the saturation of the NMR signal was not due to warming by the excitation pulse, the experiment was repeated with the exciting pulse 240 ppm above the reference frequency. In this instance both spectral lines were reduced, some saturation of the right peak did occur, but this caused a much smaller reduction than excitation at the lower frequency. We can conclude, from these experiments, that the dominate path for relaxation of the bulk ^{129}Xe is through the dipole coupling of $^{129}Xe_{Surface}$ and $^{129}Xe_{Bulk}$.

D. Cell IV - Grafoil

In order to show that the distinct features seen in the xenon NMR spectroscopy from silica gel were not due to the properties of the silica gel but instead were the properties of the xenon itself, we investigated adsorbed xenon on the surface of Grafoil® (exfoliated graphite). Carbon in the form of graphite has a simple crystalline structure consisting of layers of hexagonally arranged atoms and the exfoliated material has large atomically flat surfaces,

TABLE II: Spin lattice relaxation times for ^{129}Xe on the silica gel substrates

Cell	Xe Monolayers	T_1 for Lower Frequency Spectral Line**(surface)**	T_1 for Higher Frequency Spectral Line**(bulk)**	Ratio **T_1(bulk)/T_1(surface)**
I	0.60	2400 s	27000 s	11.3
	1.40	2830 s	37607 s	13.3
II	0.72	3000 s		
	1.63	3235 s	54165 s	16.7
III	0.74	3608 s	10412 s	2.9
	1.51	4760 s	20664 s	4.3

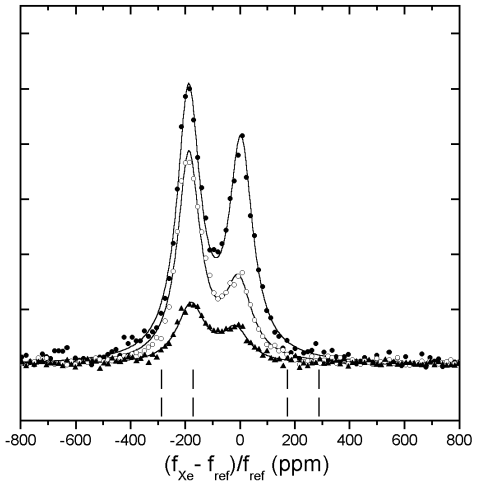

FIG. 9: • Equilibrium ^{129}Xe NMR spectra, ▲ after applying saturation pulses at -240 ppm (left dashed lines), ○ after applying saturation pulses at +240 ppm (right dashed lines).

typically 500 Å across. With this simple structure we hoped to obtain data that would improve our understanding of the xenon spectroscopy at these low temperatures and high magnetic fields. Unfortunately we encountered several obstacles in using this material. First, Grafoil has a much smaller surface area to volume ratio than silica gel, so the signal from an equivalent number of monolayers of xenon adsorbed on the surface was much smaller than with the silica gels. Secondly, graphite is an electrical conductor. Discs of Grafoil were stacked in the sample cell between discs of DuPont Kapton® polyimide film in order to try to inhibit the conductivity in the direction perpendicular to the NMR rf field. With this setup the ^{129}Xe NMR signal as well as the ^{13}C signal became visible but both were weak. The diamagnetism **of the carbon lead to a line width for the single spectral line from Grafoil of 112 kHz, which was considerably broader than for whole spectrum from silica gel (85 KHz), as seen on Fig. 10. It proved impossible to discern two peaks from the data**. The results from this investigation lacked sufficient quality to have **great** significance.

The use of Grafoil as a substrate could still provide useful information at lower magnetic fields where the effect of the diamagnetism in the carbon will be reduced. It is possible to polarize ^{129}Xe at high field and measure at low magnetic field while preserving the xenon NMR signal.

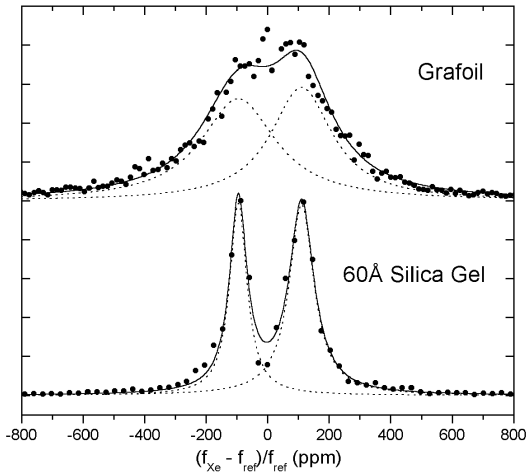

FIG. 10: Upper: ^{129}Xe NMR spectra from 1.82 monolayers of xenon adsorbed onto Grafoil at 100 mK. Lower: ^{129}Xe NMR spectra from 1.40 monolayers of xenon adsorbed onto silica gel at 100 mK.

IV. CONCLUSIONS

We have investigated the ^{129}Xe NMR spectra of xenon atoms adsorbed onto silica gel and Grafoil substrates, at extremely low temperatures and high magnetic fields. We believe that due to the high sensitivity of the ^{129}Xe NMR resonance frequency and longitudinal relaxation time to its local environment, we were able to observe separately the xenon nuclei belonging to the surface monolayer and to underlying bulk monolayers. This unique situation allowed us to examine the processes of relaxation of the

^{129}Xe, leading us to the conclusions that the predominate method of relaxation for the surface xenon atoms is through the coupling with mobile ^{3}He atoms and for the underlying ^{129}Xe, relaxation is dominated by the coupling to the surface ^{129}Xe. We also showed that with the incorporation of a silver sinter heat exchanger in the sample cell, it was possible to cool xenon to temperatures of around 10 mK in a single day; this could lead to advances in the production of hyperpolarized ^{129}Xe through the brute force technique.

V. ACKNOWLEDGMENTS

We thank Mr. P. Smith and Mr. C. Palender for their consistent engineering and technical support, and the EPSRC for their financial support.

[1] T. Pietrass and H. C. Gaede. Optically polarized ^{129}Xe in NMR spectroscopy. *Adv. Mat.*, 7:826–838, 1995.

[2] D. Raftery, H. Long, T. Meersmann, P. J. Grandinetti, L. Reven, and A. Pines. High-field nmr of adsorbed xenon polarized by laser pumping. *Phys. Rev. Lett.*, 66:584–587, 1991.

[3] V. V. Terskikh, I. L. Mudrakovskii, and V. M. Mastikhin. ^{129}Xe nuclear magnetic resonance studies of the porous structure of silica gels. *J. Chem. Soc. Faraday Trans.*, 89:4239–4243, 1993.

[4] T. Pietrass, J.M. Kneller, R. A. Assink, and M. T. Anderson. ^{129}Xe NMR of mesoporous silicas. *J. Phys. Chem. B*, 103:8837–8841, 1999.

[5] W. C. Conner, E. L. Weist, T. Ito, and J. Fraissard. Characterization of the porous structure of agglomerated microspheres by ^{129}Xe NMR spectroscopy. *J. Phys. Chem.*, 93:4138–4142, 1989.

[6] M. A. Springuel-Huet, J. L. Bonardet, A. Gédéon, Y. Yue, V. N. Romannikov, and J. Fraissard. Mechanical properties of mesoporous silicas and alumina-silicas MCM-41 and SBA-15 studied by N_2 and ^{129}Xe NMR. *Microporous and Mesoporous Materials*, 44-45:775–784, 2001.

[7] C.-J. Tsiao, K. A. Carrado, and R. E. Botto. Investigation of the microporous structure of clays and pillared clays by ^{129}Xe NMR. *Microporus and Mesoporous Materials*, 21:45–51, 1998.

[8] T. Ito and J. Fraissard. ^{129}Xe NMR study of xenon adsorbed on Y zeolites. *J. Chem. Phys.*, 76:5225–5229, 1982.

[9] J. Fraissard and T. Ito. *Zeolites*, 8:350–361, 1988.

[10] T. Rõõm, S. Appelt, and R. Seydoux. Enhancement of surface NMR by laser-polarized noble gases. *Phys. Rev. B*, 55:11604–11610, 1997.

[11] I. L. Moudrakovski, V. V. Terskikh, C. I. Ratcliffe, and J. A. Ripmeester. A ^{129}Xe NMR study of functionalized ordered mesoporous silica. *J. Phys. Chem. B.*, 106:5938–5946, 2002.

[12] A. Nossov, E. Haddad, F. Guenneau, and A. Gédéon. Application of continuously circulating flow of hyperpolarized (HP) ^{129}Xe-NMR on mesoporous materials. *Phys. Chem. Chem. Phys.*, 5:4473–4478, 2003.

[13] H. J. Jänsch, T. Hof, and U. Ruth et al. NMR of surfaces: sub-monolayer sensitivity with hyperpolarized ^{129}Xe. *Chem. Phys. Lett.*, 296:146–150, 1998.

[14] H. J. Jänsch, P. Gerhard, and M. Koch. ^{129}Xe on Ir(111): NMR study of xenon on a metal single crystal surface. *Proc. Natl. Acad. Sci. USA*, 101:13715–13719, 2004.

[15] E. R. Hunt and H. Y. Carr. Nuclear magnetic resonance of ^{129}Xe in natural xenon. *Phys. Rev.*, 130:2302–2305, 1963.

[16] D. Brinkmann and H. Y. Carr. Local magnetic field shift in liquid and solid xenon. *Phys. Rev.*, 150:174–179, 1966.

[17] M. Gatzke, G. D. Cates, B. Driehuys, D. Fox, W. Happer, and B. Saam. Extraordinarily slow nuclear spin relaxation in frozen laser-polarized ^{129}Xe. *Phys. Rev. Lett.*, 70:690–693, 1993.

[18] W. M. Yen and R. E. Norberg. Nuclear magnetic resonance of ^{129}Xe in solid and liquid xenon. *Phys. Rev.*, 131:269–275, 1963.

[19] E. V. Krjukov, J. D. O'Neill, and J. R. Owers-Bradley. Brute force polarization of ^{129}Xe. *J. Low. Temp. Phys.*, 140:397–408, 2005.

[20] N. Bišķup, N. Kalechofsky, and D. Candela. Spin polarization of xenon films at low-temperature induced by ^{3}He. *Physica B*, 329:437–438, 2003.

[21] A. K. Jameson, C. J. Jameson, and H. S. Gutowsky. Density dependence of ^{129}Xe chemical shifts in mixtures of xenon and other gases. *J. Chem. Phys.*, 53:2310–2321, 1970.

[22] E. V. Krjukov, J. D. O'Neill, and J. R. Owers-Bradley. To be published. *Proceedings of the 24th International Conference on Low Temperature Physics.*